Available online at www.sciencedirect.com
SCIENCE DIRECT
Virology 349 (2006) 335–346
VIROLOGY
www.elsevier.com/locate/yviro

Human coronavirus OC43 infection induces chronic encephalitis leading to disabilities in BALB/C mice

Hélène Jacomy [a], Gabriela Fragoso [b], Guillermina Almazan [b], Walter E. Mushynski [c], Pierre J. Talbot [a,*]

[a] *Laboratory of Neuroimmunovirology, INRS-Institut Armand-Frappier, 531 boulevard des Prairies, Laval, Québec, Canada H7V 1B7*
[b] *Department of Pharmacology and Therapeutics, Montreal, Quebec, Canada H3G 1Y6*
[c] *Department of Biochemistry McGill University, Montreal, Quebec, Canada H3G 1Y6*

Received 8 November 2005; returned to author for revision 11 January 2006; accepted 18 January 2006
Available online 9 March 2006

Abstract

The notion that an infectious respiratory pathogen can damage the central nervous system (CNS) and lead to neurological disease was tested using a human respiratory coronavirus, the OC43 strain of human coronavirus (HCoV-OC43). First, primary cell cultures were used to determine the susceptibility of each type of neural cells to virus infection. Neurons were the target cells, undergoing degeneration during infection, in part due to apoptosis. Second, neuropathogenicity was investigated in susceptible mice. Intracerebral inoculation of HCoV-OC43 into BALB/c mice led to an acute encephalitis with neuronal cell death by necrosis and apoptosis. Infectious virus was apparently cleared from surviving animals, whereas viral RNA persisted for several months. Some of the animals surviving to acute encephalitis presented an abnormal limb clasping reflex and a decrease in motor activity starting several months post-infection. These results suggest that viral persistence could be associated with an increased neuronal degeneration leading to neuropathology and motor deficits in susceptible individuals.

Keywords: Human coronavirus; Coronavirus; OC43; HCoV-OC43; Neurodegeneration; Chronic encephalitis; Apoptosis; Persistence; Motor disabilities

Introduction

Human coronaviruses (HCoV), designated as strains HCoV-OC43 (group 2) and HCoV-229E (group 1), are recognized respiratory pathogens responsible for up to one third of common colds (McIntosh, 1996; Myint, 1994), as well as nosocomial infections (Sizun et al., 2000). They have occasionally been associated with other pathologies, such as pneumonia, meningitis, enteritis (Resta et al., 1985; Riski and Hovi, 1980), and more recently in acute disseminated encephalomyelitis (Yeh et al., 2004). During the 2002–2003 epidemic of Severe Acute Respiratory Syndrome (SARS), a novel coronavirus (SARS-CoV) was identified as the etiological agent of SARS (Peiris et al., 2003). Its nucleotide sequence presents some degree of homology with coronaviruses of groups 1 and 3 (Rest and Mindell, 2003) but mostly with group 2 (Snijder et al., 2003). The complete genome sequence of SARS-CoV shows 53.1% identity with HCoV-OC43 (St-Jean et al., 2004). Even though SARS is mainly characterized by a pulmonary infection with high infectivity and fatality (Nie et al., 2003), SARS-CoV RNA was detected in the cerebrospinal fluid of patients (Hung et al., 2003; Lau et al., 2004), and SARS-CoV-positive cells were reported in autopsied brain samples by in situ hybridization (Ding et al., 2004). More recently, infectious virus was detected in brain tissue of a SARS patient (Xu et al., 2005). These reports are consistent with neuroinvasive properties of this virus, as it has been reported for other HCoV strains (Arbour et al., 2000; Burks et al., 1980; Murray et al., 1992; Stewart et al., 1992; Yeh et al., 2004). Furthermore, the neuroinvasive properties of SARS-CoV were recently reported in mouse CNS (Glass et al., 2004). Thus, a neurotropic and neuroinvasive virus entering the brain could directly trigger neurodegeneration and/or initiate a CNS-directed inflammatory process leading to central nervous system (CNS) damage. HCoV may thus be involved in neurological disorders.

* Corresponding author. Fax: +1 450 686 5566.
E-mail address: pierre.talbot@iaf.inrs.ca (P.J. Talbot).

0042-6822/$ - see front matter © 2006 Elsevier Inc. All rights reserved.
doi:10.1016/j.virol.2006.01.049

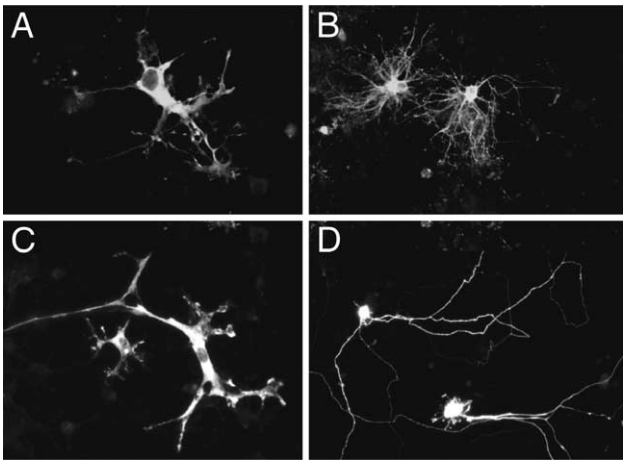

Fig. 1. Susceptibility of each type of neural cells to HCoV-OC43 infection. Immunofluorescent labeling demonstrated that HCoV-OC43 proteins were found in almost pure cultures of astrocytes (A), oligodendrocytes (B), microglial cells (C), and neurons (D).

We previously reported the development of a mouse model to characterize HCoV-OC43-mediated neuropathogenesis in vivo (Jacomy and Talbot, 2003). Infection by HCoV-OC43 was dependent on the route of inoculation, viral dose, the age, and the strain of mouse. When virus reached the CNS, infected mice developed acute encephalitis resulting from neuronal infection. We now report that some neurons underwent apoptosis during the acute phase of disease, and that some infected mice survived the infection and presented motor disabilities associated with viral persistence in CNS and loss of neurons in the brain.

In order to better understand the neuropathological effects of HCoV-OC43 infection, we have also developed cultures of different rodent neural cell populations. Moreover, we also investigated the infectious properties of HCoV-OC43 Paris, a recently isolated respiratory variant of HCoV-OC43, which has never been propagated in murine cells or even neural cells, unlike the original ATCC strain. A combination of specific cell markers and virus-specific reagents was used to determine which cell types were susceptible to HCoV-OC43 infection. Glial cells alone were shown to be susceptible to viral infection, but only in a nonproductive fashion, whereas neurons were productively infected and were definitively identified as viral targets. We further demonstrate that part of the virus-induced neuronal death results from apoptosis, both in vitro and in vivo.

Therefore, neuronal cell death induced by HCoV-OC43 and associated with viral persistence and activation of microglial cells may play a major role in CNS impairment in surviving animals, and apoptosis may contribute to the cytotoxicity associated with viral infection.

Results

Infection of purified rat neural cell populations in culture

Using single immunofluorescence staining of almost pure (more than 90%) neural cell cultures, HCoV-OC43 viral proteins were shown to be expressed in microglia, astrocytes, oligodendrocytes, as well as neurons, as soon as 24 h post-infection (Fig. 1). Numerous dorsal root ganglion (DRG)-neurons in neuron-enriched cultures (Fig. 2), or DRG-neurons with Schwann cells (SC) (data not shown), were infected. Cytopathic effects (CPE) were observed after viral infection, especially in pure DRG-N cultures. Infected DRG-N exhibited signs of degeneration, starting with the formation of retraction balls, beading of axons, and loss of oriented axonal neurites (Fig. 2, D and E), whereas axonal neurites of noninfected neurons were more linear and showed no beading (Fig. 2, F). Moreover, after infection, neurons appeared to be more aggregated, with fewer axonal neurites as compared to neurons in the noninfected wells (Fig. 2: compare B and F). In DRG-N/SC, cytopathic effects were less pronounced, although some infected neurons did exhibit beading and nonlinearity of axonal neurites (data not shown). Double immunofluorescence staining confirmed that mainly neurons were susceptible to viral infection in DRG-N/SC cultures. Occasionally, a few SCs were positive for viral antigens (data not shown).

Infectious viral titers were determined in culture media from different cell types. After infection by HCoV-OC43, no infectious virus was detected in almost pure oligodendrocyte and astrocyte cell culture supernatants until 3 weeks post-infection. The infectious virus titer expressed in $TCID_{50}$/ml was $\leq 10^{0.5}$, which constitutes the threshold of sensitivity of the

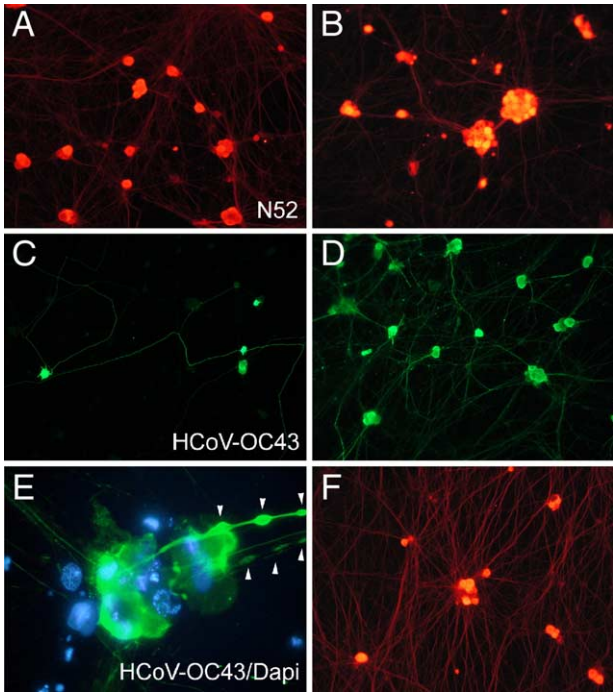

Fig. 2. Viral infection and cytopathic effects of DRG-N cultures. At 2 days post-infection (dpi), numerous DRG-neurons were present (A), and only a few were infected (C). At 8 dpi, neurons were still present in the infected culture (B) and were densely packed. Numerous neurons were infected at 8 dpi (D). (E) A succession of expansions and constrictions can be seen in infected axons of these unmyelinated fibers (arrowheads point towards axonal beading). (F) Noninfected culture showing less densely packed neurons, with numerous axonal processes as compared to the infected culture (B). Original magnification: ×100, except panel E: original magnification: ×400.

assay. Therefore, astroglial and oligodendroglial cells could be infected but did not sustain a productive infection. Microglia produced a very low viral titer ($10^{0.75}$ at 1 week to $10^{1.25}$ $TCID_{50}$/ml at 3 weeks post-infection). In pure DRG-N cell cultures, a low viral titer of $10^{1.25}$ to 10^{2} $TCID_{50}$/ml was measured during the first week post-infection, whereas a very significant viral titer was found in mixed cultures of DRG-N/SC, reaching $10^{3.75}$ $TCID_{50}$/ml.

Infection of primary neural cell cultures from hippocampus and cortex

Given that the same results were obtained after viral infection of rat or mouse primary cell cultures, only results obtained with mouse cells are presented herein.

Neuronal cells cultures

In hippocampal and cortical cultures enriched (more than 85%) in neuronal cells, astrocytes were also present (around 10%) and formed a feeding layer permitting the growth of neurons. Microglial cells were also present in this culture and represented less than 5% of the cells. During the first 24 h post-infection, only neurons sustained viral infection (Fig. 3A). After 2 days, neurons and astrocytes were found positive for viral antigens (Fig. 3B), and after 7 days, most of the neurons had disappeared from the infected cultures. While neurons in noninfected cultures were still present, numerous activated microglial cells were found close to infected cells (Fig. 3C). Measurement of infectious viral titers in the supernatants during the first week revealed that these cultures produced significant viral titers (Fig. 4A). Moreover, the two variants of HCoV-

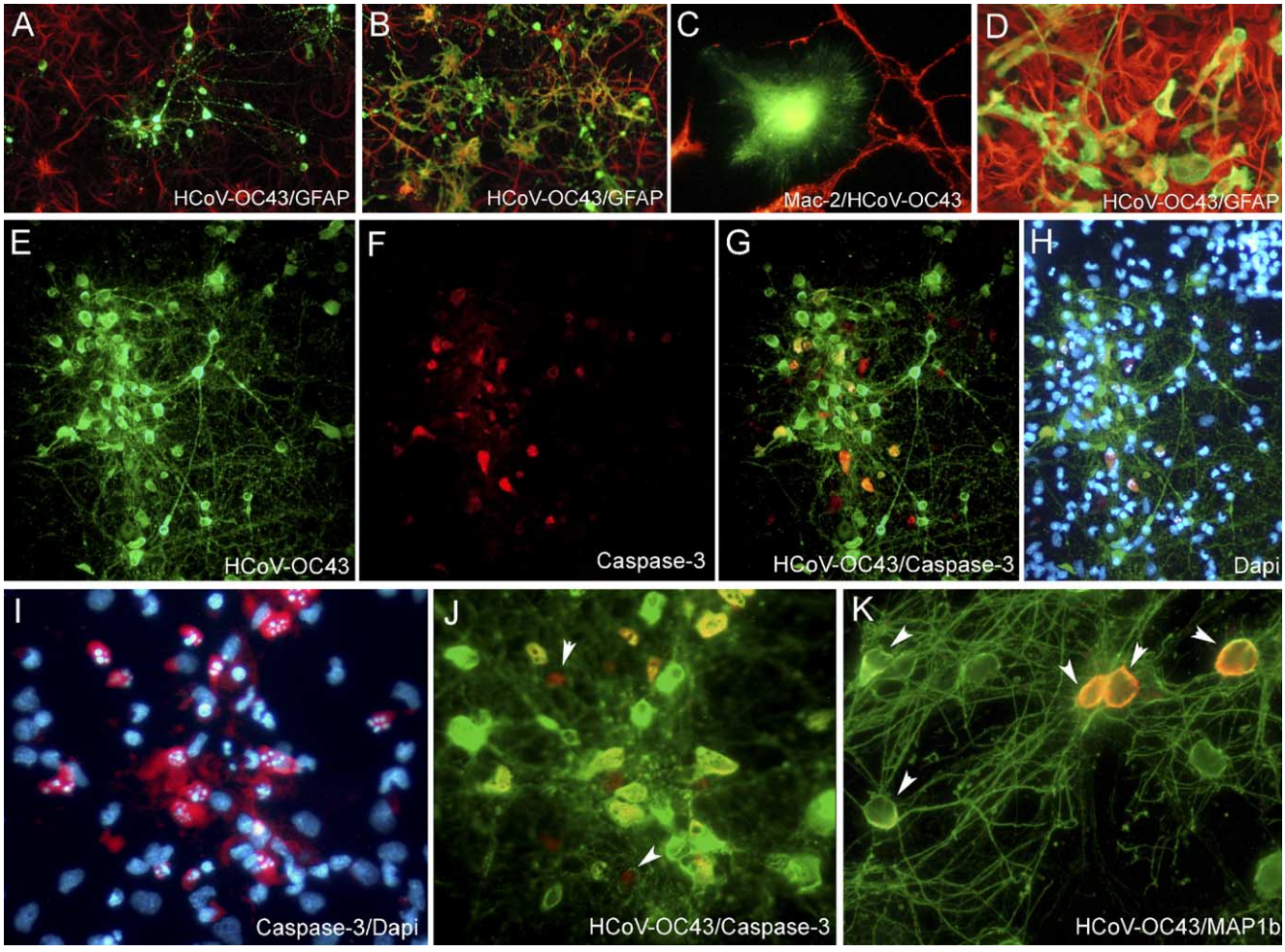

Fig. 3. HCoV-OC43 tropism and induction of apoptosis in mouse cortical or hippocampal cultures. (Panels A and B) Neuronal cell cultures were double stained for HCoV-OC43 (in green) and for astrocytes (in red). At 1 day post-infection (A), only neuronal cells were positive for virus, whereas at 3 dpi (B), several astrocytes were also double stained. (C) An activated microglial cell (in green) was in close proximity with infected axonal prolongations (in red). (D) Glial cortical cultures contained numerous astrocytes (in red) with some of them double stained with MAbs against HCoV-OC43 (in green). (E–K) Apoptotic death of primary CNS neurons. (E–H) Cortical cell cultures containing numerous infected cells (E) and some activated caspase-3-positive cells (F). The merged picture in panel G shows that most activated caspase-3-positive cells were infected (yellow). Adding DAPI staining to the merged picture shown in panel G (H) showed that numerous noninfected cells were also present in this field. (I–K) Primary hippocampal cell cultures infected by HCoV-OC43. Activated caspase-3 staining and fragmented nuclei revealed by DAPI-staining were perfectly colocalized (I). In the same field, merging activated caspase-3 (red) and antiviral staining (green) revealed that most of the activated caspase-3-positive cells were infected (yellow), although some were not (appearing red, arrowheads). In panel K, merging of neuronal staining (green) and antiviral staining (red) confirmed that infected cells (arrowheads) were neurons. Original magnification: ×100 for panels A, B, E–H, ×200 for panels D, I–J and ×400 for panels C and K.

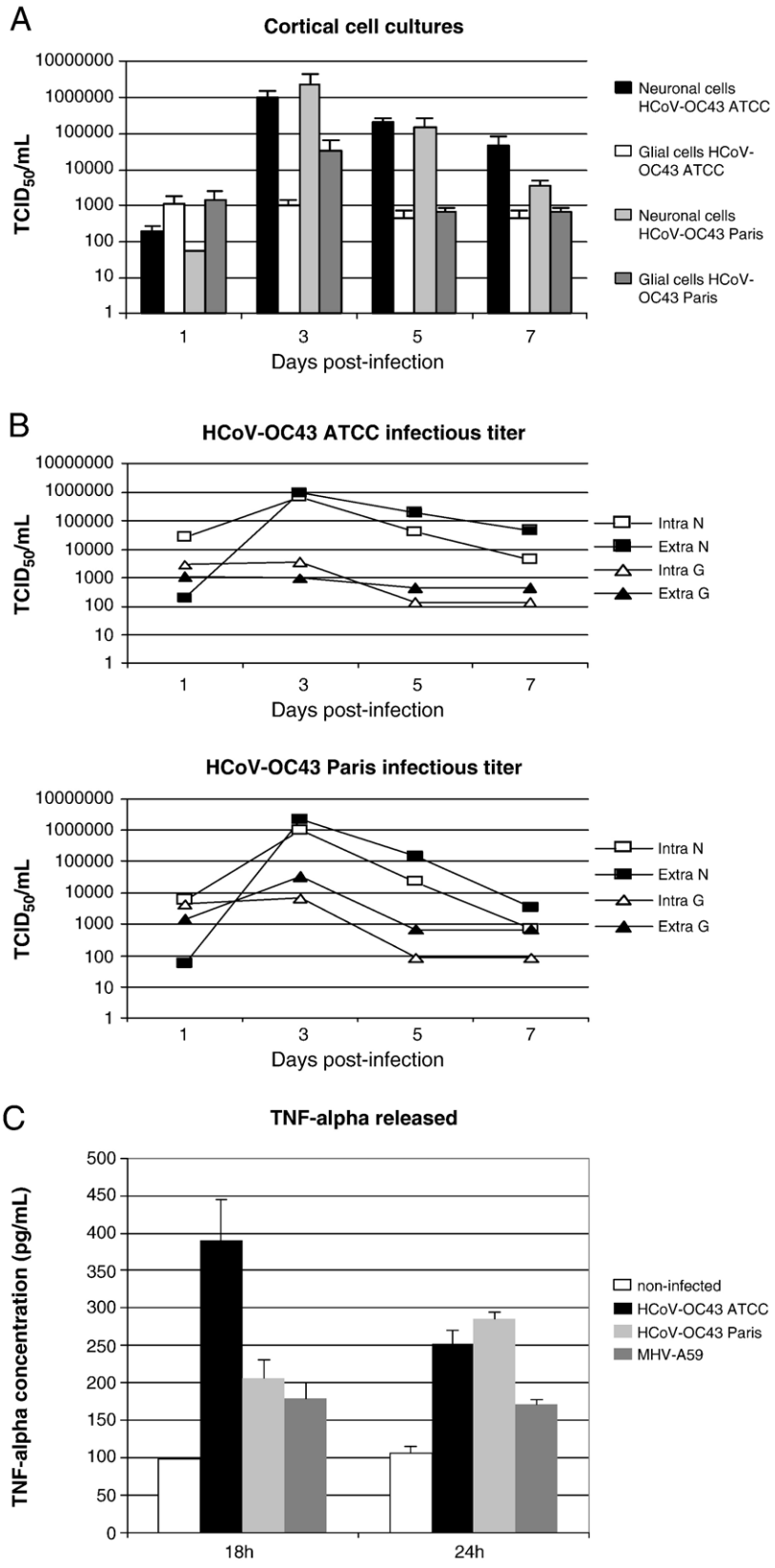

Fig. 4. Viral replication and release of TNF-α by CNS cells. (A) Infectious viral titers in infected neuronal or glial cortical cell cultures after HCoV-OC43 ATCC and HCoV-OC43 Paris infections. Replication levels in neuronal cells increased during the first days of infection, reaching a maximum at around 3 days post-infection. At that time, cytopathic effects in cultures increased and numerous neurons were dead. Replication levels in glial cell cultures were less pronounced than in neuronal cell cultures for both HCoV-OC43 strains. (B) Infectious viral titers in supernatant versus intracellular bodies of infected neuronal (N) or glial (G) cortical cell cultures after HCoV-OC43 ATCC and HCoV-OC43 Paris infection. (C) TNF-α release after HCoV-OC43 infection of neuronal cells. HCoV-OC43 ATCC infected neuronal cell cultures released a high amount of TNF-α in the supernatant.

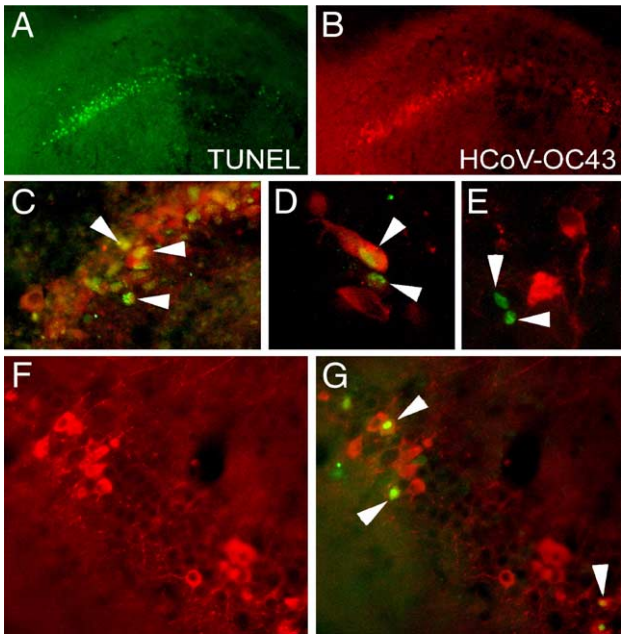

Fig. 5. Apoptosis during acute encephalitis. TUNEL staining (A) at 11 days post-infection (dpi) was evident in the CA1 hippocampal layers, and the same region was positive for viral antigen (B), and the merged picture (C) illustrates that some neurons (arrowheads) underwent apoptosis. At a higher magnification, some infected neurons were positive for TUNEL staining (arrowheads, panel D), whereas some noninfected cells with hallmarks of apoptotic death (arrowheads, panel E) were located close to infected cells (in red, panel E). In CA3 hippocampal layers, some infected cells (F) also exhibited apoptotic cell death as shown on the merged figure (arrowheads, panel G). Original magnification: ×100 for panels A and B, ×400 for panels C to D.

OC43 used in this study were able to replicate in rodent (mice or rats) CNS cell cultures. HCoV-OC43 ATCC and HCoV-OC43 Paris produced infectious virus and had similar temporal infection pattern (Fig. 4A).

Glial cell cultures

In glial cultures from hippocampal or cortical cells, viral antigens were found in astrocytes (Fig. 3D). Measurement of infectious titers for the two HCoV-OC43 variants in the supernatants, during the first week, revealed that these cultures produced significant viral titers, even though lower than in enriched neuronal cultures (Fig. 4A).

In order to investigate whether HCoV-OC43 ATCC or HCoV-OC43 Paris virions were trapped in cell bodies of glial cells, we measured the infectious viral titer in the intra- versus extracellular space of neuronal (N) versus glial (G) cell cultures (Fig. 4B). For both neuronal and glial cortical cell cultures, no significant differences were found. At approximately 3 dpi, the levels of infectious virus were higher in the extracellular space for both cell cultures, indicating that virus was not trapped in glial cell bodies (Fig. 4B).

Apoptosis in neuronal cell culture

Immunofluorescent staining revealed that after infection of hippocampal and cortical cultures, cells were positive for activated caspase-3 (Figs. 3E–J). The nuclear fragmentation/

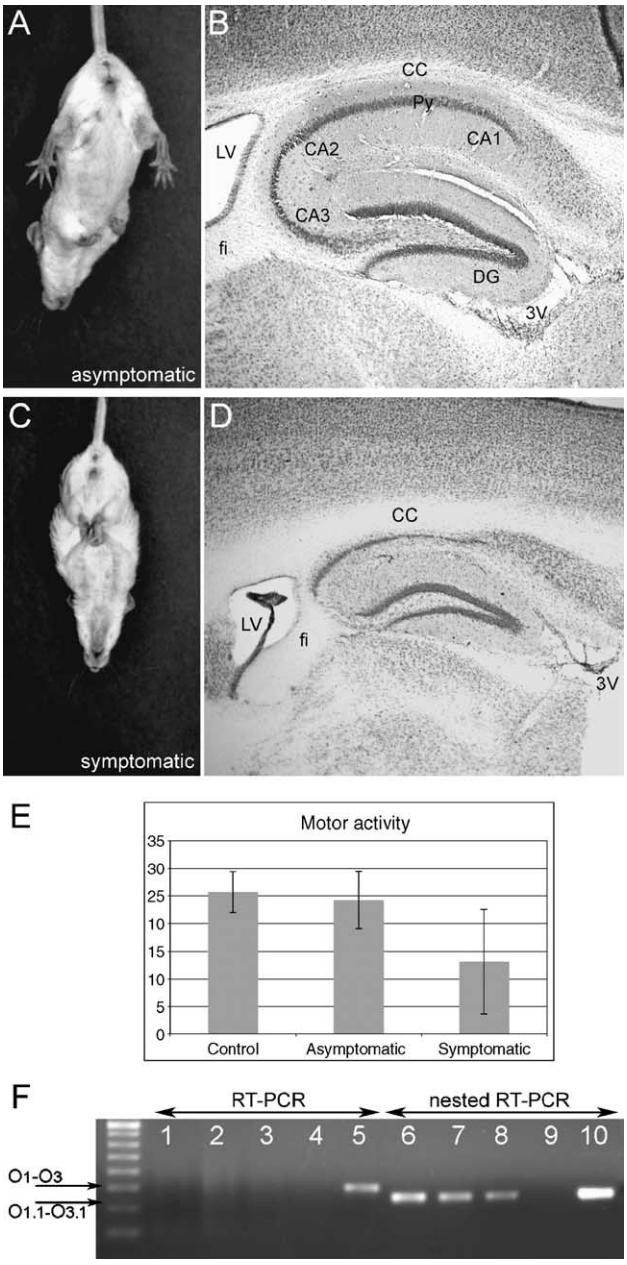

Fig. 6. HCoV-OC43-mediated pathogenesis in BALB/c mice. When suspended by the tail, asymptomatic HCoV-OC43-infected BALB/c mice (A) extended their legs, whereas symptomatic HCoV-OC43-infected mice presented abnormal flexion of the four limbs (C). (B and D) Cresyl violet staining of a hippocampus from a control (B) and an infected (D) mouse. Animals surviving the acute HCoV-OC43 infection were histologically examined 1 year later and showed a hippocampus smaller than noninfected or asymptomatic animals (Py: pyramidal cell layers; DG: dentate gyrus; fi: fimbria of hippocampus; cc: corpus callosum; LV lateral ventricle; 3V: third ventricle). (E) Motor activity (means ± SEM) of control, asymptomatic and symptomatic groups of mice in the open field test. The observer registered the number of times the animals entered completely into each square (counts/5 min). (F) Detection of HCoV-OC43 RNA in the brain of symptomatic BALB/c mice inoculated intracerebrally with $10^{4.5}$ $TCID_{50}$ of HCoV-OC43. Although RT-PCR analysis with primer pairs O1–O3 did not detect HCoV-OC43 RNA, nested primer pairs O1.1–O3.1 did show the presence of HCoV-OC43 RNA. Lanes 1, 2, 3, and 6, 7, 8: surviving mice 1 year post-infection; lanes 4 and 9: noninfected mice; lanes 5 and 10: positive-control HCoV-OC43 infected HRT-18 cells.

condensation observed with DAPI staining colocalized with activated caspase-3-positive cells (Fig. 3I), confirming that an apoptotic process was taking place in the infected cell cultures. As demonstrated by double immunofluorescent staining, some infected cells were also positive for activated caspase-3 (Figs. 3E–G and J), indicating that viral infection could directly trigger an apoptotic response. Ten to fifteen percent of infected cortical cells and more than 20% of infected hippocampal cells underwent apoptosis. Double labeling for neuronal and viral antigens confirmed that the infected cells were neurons (Fig. 3K, arrowheads). Interestingly, around 5% of activated caspase-3-positive cells did not contain viral antigens but were close to infected cells, suggesting that infected neurons or adjacent astrocytes or activated microglial cells may have released soluble mediators that could induce apoptosis in noninfected cells (Fig. 3J).

We also investigated TNF-α release after HCoV-OC43 infection, since it is a pro-inflammatory cytokine produced primarily in response to viral infection and which directly regulates innate immunity and viral pathogenesis (Guidotti and Chisari, 2001; Herbein and O'Brien, 2000) and was shown to be upregulated after MHV infection (Rempel et al., 2005). Cell cultures infected by HCoV-OC43 ATCC released a high amount of TNF-α in the supernatant (Fig. 4C), as compared to noninfected cells or to identical primary cell cultures infected by HCoV-OC43 Paris or MHV-A59, the latter used as a positive control (Li et al., 2004). The synthesis of TNF-α was very fast, as 400 pg/ml of TNF-α was detected as soon as 18 hpi.

Infection of mice

To confirm the biological relevance of these in vitro observations, we determined whether viral infection of mouse CNS could also induce neuronal apoptosis. As previously reported, intracerebral inoculation of HCoV-OC43 into mice led to a generalized infection of the CNS, which also affected the hippocampus (Jacomy and Talbot, 2003). Mice recovering from infection were all found to be seropositive for HCoV-OC43, confirming that they were indeed infected (data not shown). Double immunostaining for viral antigens and TUNEL assays were performed on brain sections during the acute phase of the encephalitis at 11 days post-infection (11 dpi). Isolated TUNEL-positive cells could be seen in the cortical area and the striatum: in these regions, most of the infected cells did not show the hallmarks of apoptosis. In the hippocampus, some neurons in the CA1 and some in the CA3 layers were TUNEL-positive, and numerous cells, in the same region, were also positive for viral antigens (Fig. 5, panels A–B and F–G). The merged pictures illustrate that some of the infected neurons underwent apoptosis (Fig. 5, panels C, D, and G), and that noninfected cells localized near the infected ones were also undergoing apoptosis (Fig. 5, panel E). After an intracerebral inoculation of 10 μl of an HCoV-OC43 virus stock containing 10^6 $TCID_{50}$/ml, about 80% of BALB/c mice survived. From 6 months to a year post-infection, some of these surviving animals exhibited abnormal reflexes (limb clasping). When normal mice were suspended by the tail, they extended their legs, whereas infected mice reflexively contracted their four limbs (Figs. 6, panel C). At 6 months post-infection, 9 of the 29 surviving mice presented limb clasping, and at 1 year post-infection, 7 of the 21 remaining animals did. Thus, limb clasping affected about 30% of the surviving BALB/c mice. Mice with abnormal reflexes (clasping) were classified as symptomatic and mice with normal reflexes were classified as asymptomatic. Moreover, symptomatic animals presented clinical signs of decreased activity in an open field test (Fig. 6E). A decreased number of counts was considered to represent a decrease in locomotor activity. Indeed, symptomatic mice showed hypoactivity and a decreased exploration pattern, as sniffing and sifting were markedly diminished, as compared to asymptomatic or normal mice. One year post-infection, cresyl violet staining of the CNS of symptomatic surviving mice revealed that the hippocampus was smaller in size, with hippocampal cell layers less dense than in control or asymptomatic mice (Figs. 6B and D) and also presented reduced CA1 and CA3 hippocampus fields. Neuronal apoptosis and necrosis taking place during the acute phase of the disease could explain only part of the tissue loss of hippocampal gyrus observed in infected mice which survived to the acute virus-induced encephalitis, as demonstrated by the observation of hippocampal regions, 6 months post-infection, where neuronal loss in hippocampal layers were less pronounced (Fig. 7). Moreover, some brains treated for histological staining revealed infiltration and activated microglia spreading into different CNS regions, especially in the hippocampus (Fig. 8), illustrating the chronic state of the disease. Whereas no viral antigens could be detected, viral

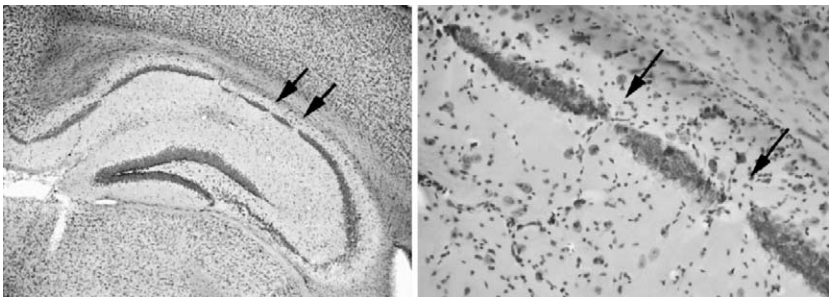

Fig. 7. Chronic encephalitis and neuronal loss in hippocampus, 6 months post-infection. Scattered damage of CA1 neuronal cell layers was observed (arrows). Disruption of the neuronal CA1 layer is more evident at higher magnification (right panel). Original magnification, ×40 (left panel) and ×200 (right panel).

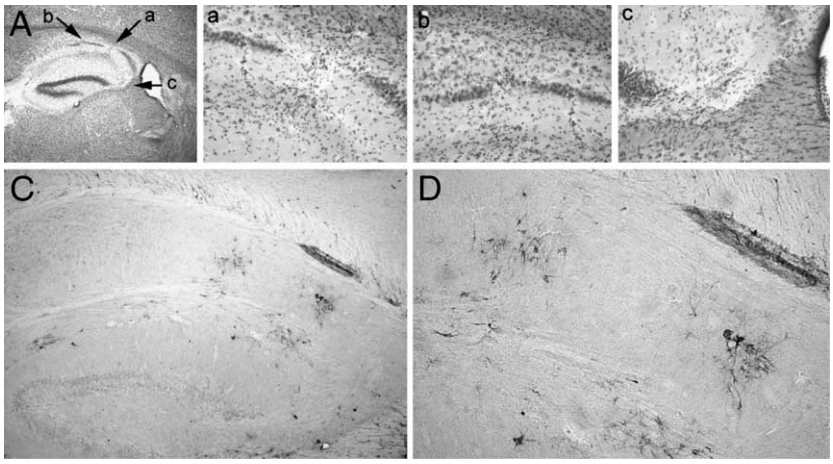

Fig. 8. Chronic encephalitis and neuronal loss in hippocampus, 1 year post-infection. (A) Cresyl violet staining revealed neuronal loss in CA1 and CA3 hippocampal cell layers (arrows). Original magnification, ×40. Magnification of damaged regions (a–c) illustrates neuronal loss on CA1 and CA3 hippocampal layers and the presence of infiltrating cells (magnification, ×200). Panel C and magnification on panel D: cluster of activated microglia. Original magnification, ×100 (C) and ×200 (D).

mRNA could be detected in some symptomatic mice using a nested RT-PCR assay (Fig. 6F) but remained undetectable in asymptomatic mouse brains. As previously reported (Jacomy and Talbot, 2003), RT-PCR amplification of the HCoV-OC43 N RNA with primer pairs O1–O3 was not sensitive enough to demonstrate viral persistence in mouse brain, although this has now been achieved with a more sensitive nested RT-PCR technique, using the O1.1–O3.1 nested primer pairs (Fig. 6F).

Discussion

Neurons are, until they die, the major target of HCoV-OC43 in primary hippocampal or cortical cells cultures representative of in vivo brain cells, unlike MHV (Nakagaki et al., 2005; Sun and Perlman, 1995). Almost pure astroglial and oligodendroglial cell cultures only sustained an abortive HCoV-OC43 infection, as previously reported (Pearson and Mims, 1985; Bonavia et al., 1997). Microglial cells were productively infected, albeit with a very low viral titer, as we have described for primary human adult microglia (Bonavia et al., 1997). Previous studies targeting neurons have indicated susceptibility to HCoV-OC43 infection of immortalized neuronal cell lines (Arbour et al., 1999; Collins, 1995), as well as neurons in primary cultures of mouse DRG (Pearson and Mims, 1985). The current study extends these previous reports by showing that the respiratory human coronavirus HCoV-OC43 has a preferential tropism for neurons, and that it induces cytopathic effects after establishing a productive infection of these cells. Axons of infected neurons exhibited a typical beaded pattern, a result of the underlying pathology. Beading constrictions are due to changes in the cytoskeleton (Ochs et al., 1996), and microtubules disruption could constitute a major process in the apoptotic response (Mollinedo and Gajate, 2003). Oxidative stress has also been associated with axonal swelling developing into axonal beading (Roediger and Armati, 2003).

Interestingly, DRG-N, which allowed the use of an almost pure neuronal culture, did not present signs of apoptotic neuronal cell death and produced fewer viral particles than hippocampal or cortical neurons, indicating the possibility of an internal determinant of CNS versus peripheral nervous system (PNS) susceptibility or a more probable synergy between cells, such as the release of mediators like gamma interferon (Collins, 1995) or tumor necrosis factor-alpha (Robertson et al., 2001). In glial cortical cell cultures, a measurable infectious viral titer was produced, whereas almost pure astrocytes or oligodendrocytes cultures failed to release infectious viral particles. This is consistent with a synergy between glial cells: astrocytes, microglia, and fibroblasts could release soluble factors such as cytokines or chemokines which may induce changes in cell surface receptors and transcription factors that favor viral entry and productive replication. Indeed, it was reported that HIV may infect cells that do not express receptors for viral entry (Rozmyslowicz et al., 2003), and that stress could influence the immune response and alter the pathophysiology of infection (for review, see Padgett and Glaser, 2003).

The HCoV-OC43 Paris variant, obtained recently from the nasal secretions of a patient showing an upper respiratory tract infection, was never passaged in mouse brains or cells, in contrast to the ATCC isolate from the 1960s. Comparison of HCoV-OC43 ATCC versus HCoV-OC43 Paris variants indicated that HCoV-OC43 possesses an intrinsic neurotropism. Neuroinvasive properties of HCoV-OC3 Paris were demonstrated in young mice (St-Jean et al., 2004). On the other hand, 21 DPN C57Bl/6 mice were more resistant to intracerebral inoculation of HCoV-OC43 Paris, as only a higher dose ($\times 10^5$) could induce acute encephalitis. Moreover, 21 DPN BALB/c were totally resistant to a viral dose of $10^{5.5}$ $TCID_{50}$ (data not shown).

We have now demonstrated for the first time that some neurons infected by HCoV-OC43 undergo apoptosis leading to cell death. Caspases are the principal executors of apoptotic cell death, and caspase-3 was identified as a key mediator in mammalian cells (Nicholson et al., 1995). We show that coronavirus-induced apoptosis involved DNA fragmentation

and caspase-3 activation, and that some noninfected cells, in close proximity to infected ones, also stained for apoptotic markers, suggesting that infected cells or adjacent glial cells, activated by the infection, secreted molecules that induce death signals in noninfected cells. Activated microglial cell are known to be one of the major source of TNF-α (Gimsa et al., 2000; Guidotti and Chisari, 2001), which can induce neuronal apoptosis (Robertson et al., 2001; Shi et al., 1998; Talley et al., 1995). We show here that HCoV-OC43-infected cultures rapidly released a high amount of TNF-α that could be responsible for at least part of the apoptosis observed in neighboring noninfected neurons. Further understanding of how TNF-α participates in viral pathogenesis remained to be clarified.

Twenty-one DPN mice infected by intracerebral inoculation of HCoV-OC43 developed signs of acute encephalitis (Jacomy and Talbot, 2003). Even though most of the infected cells degenerated after vacuolation (Jacomy and Talbot, 2003), we now report that, during the acute phase of the disease, some of the infected and noninfected neurons underwent apoptosis, especially in the hippocampal layers. Theiler's murine encephalomyelitis virus (Rubio et al., 2003) and Sindbis virus (Kimura and Griffin, 2003) were also reported to induce apoptosis, with most of the infected cells not showing hallmarks of apoptosis, as we also observed following HCoV-OC43 infection. The murine counterpart of HCoV-OC43, MHV, was also reported to induce apoptosis in mouse brain (Chen and Lane, 2002; Wu and Perlman, 1999; Schwartz et al., 2002). Apoptosis induced by coronaviral infection could be associated with HCoV-mediated neuropathogenesis by killing cells or by disseminating virus while limiting inflammatory responses. Indeed, neuronal apoptosis seems to represent an important contributing factor to acute CNS injury in humans after viral infection (DeBiasi et al., 2002; Nakai et al., 2003) and in HIV-associated dementia (Garden, 2002; Kolson, 2002).

In vivo, HCoV-OC43 inoculation resulted in a productive and cytotoxic infection of neuronal cells in mouse CNS (Jacomy and Talbot, 2003). Nevertheless, 80% of BALB/c mice survived the acute infection and around 30% of them developed limb clasping, associated with reduced locomotor activity. The pathogenic process leading to this outcome was difficult to study since an unpredictable and small percentage of mice survived the acute disease and developed these clinical symptoms of neurologic disorder. The four-limb clasping observed in some BALB/c mice surviving to HCoV-OC43 infection was similar to that previously described in various mouse models of neurodegenerative diseases (Côté et al., 1993; Reddy et al., 1998; Yamamoto et al., 2000; Guy et al., 2001). However, spinal cord examination of surviving BALB/c mice did not reveal either noticeable motoneuronal loss or inclusion or accumulation of neurofilaments in cell bodies that could account for the observed hypoactivity.

Although histological analysis of mouse brain performed 1 year post-infection failed to detect HCoV-OC43 antigens, some of the animals showed neuronal cell loss, especially in the hippocampal region, and sometimes, clusters of gliosis were disseminated in the CNS. Histological examination of hippocampal layers revealed that neuronal cell loss was more severe than what was observed during the acute phase of the disease or histological examination performed at 6 months post-infection. During the active phase of encephalitis, neuronophagia, activated microglial cells and perivascular lymphocytic infiltrates were present. In the more chronic phase, evidence of neuronal loss predominated and was sometimes associated with gliosis. Presumably, toxic compounds released by activated microglial cells could cause a nonspecific immune destruction of neurons (McGeer and McGeer, 2002). Long-term pathologic changes in the hippocampus were also described after Sindbis virus infection (Kimura and Griffin, 2003). In the current study, the decreased density of neuronal layers of the hippocampus apparently correlated with viral persistence in the brain, as monitored by the presence of viral RNA. A reduced hippocampus could trigger deficits in higher neurological functions such as learning and memory, in addition to neurological disabilities observed in these animals. Interestingly, a growing number of human studies have shown dramatic alterations in learning, memory, attention, and motor functions following cytokine treatments (Connor and Leonard, 1998).

Overall, our study is consistent with the possibility that respiratory pathogens with a neurotropic and neuroinvasive potential could cause neurodegeneration in susceptible individuals. Even though mice are not the natural host for HCoV-OC43 infections, they may contribute to our understanding of the underlying mechanisms and neuropathological consequences of coronavirus infections in humans. Furthermore, recent reports on the presence of SARS-CoV in patient brains are consistent with neuroinvasive properties of SARS-CoV in humans (Hung et al., 2003; Lau et al., 2004; Ding et al., 2004; Xu et al., 2005). The current study provides the first in vitro and in vivo experimental evidence directly supporting a causal role for a human respiratory virus in CNS pathogenesis, suggesting the importance of efforts towards investigating CNS infection by coronaviruses.

Materials and methods

Virus

The ATCC strain of HCoV-OC43 was originally (in the mid-1980s) obtained from the American Type Culture Collection (ATCC VR-759), plaque-purified and grown on the human rectal carcinoma cell line HRT-18 as previously described (Mounir and Talbot, 1992). The HCoV-OC43 Paris strain was directly isolated from a respiratory sample from a patient and grown on the human rectal carcinoma cell line HRT-18, as described (St-Jean et al., 2004). The fifth passage of HCoV-OC43 ATCC and eighth passage of Paris virus stocks (10^6 $TCID_{50}$/ml) were kept at −80 °C and were used to perform the infections. The MHV-A59 virus strain used in these experiments was propagated on DBT cells as previously described (Daniel and Talbot, 1987). Titers of infectious virus were determined by plaque assay on DBT cells (Yokomori and Lai, 1992).

Dorsal root ganglion neurons (DRG-N) and Schwann cell (SC) cocultures and purified DRG-N

Purified DRG-N/SC cocultures were prepared using methods described previously (Giasson and Mushynski, 1996). DRGs were obtained from Sprague–Dawley rat embryos (Charles River Laboratories) at 15 to 16 days of gestation. Embryos were collected in Leibovitz's (L-15) medium (Sigma-Aldrich), the spinal column was dissected from each embryo, and DRGs were plucked from the spinal cords and collected in fresh L-15 medium. DRGs were dissociated with trypsin [0.025% (w/v) in Hank's balanced salt solution (HBSS; Invitrogen)] at 37 °C for 15 min, followed by treatment with soybean trypsin inhibitor (5 mg/ml (Sigma-Aldrich) in L-15 medium). The dissociated cells were suspended for plating in defined medium consisting of DMEM/F12 (Dulbecco's modified Eagle medium (DMEM)/Ham's F12 medium; Invitrogen) containing N1 supplement (Sigma-Aldrich), 0.09% (w/v) BSA, 12 ng/ml 2.5S nerve growth factor (NGF 2.5S; Prince Laboratories) and antibiotics (penicillin/streptomycin), and cells from 3 DRGs were plated onto rat tail collagen-coated 24-well plates. The anti-mitotic agents, 5-fluoro-2′-deoxyuridine and cytosine-β-D-arabinofuranoside (Sigma-Aldrich), were used at concentrations of 10 μM to get pure neuronal cell cultures. The protocol involved two 3-day anti-mitotic treatments, beginning the day after cell plating and separated by a 3-day period in normal medium. Cell cultures were maintained in serum-free N1 medium until their use after 21 days in culture.

Glial cell cultures

Primary cultures of different glial cell populations were prepared from the brains of newborn Sprague–Dawley rats as previously described (Almazan et al., 1993; McCarthy and de Vellis, 1980). The meninges and blood vessels were removed from the cerebral hemispheres into F12 medium. After the last filtration of tissue suspension through a 150-μm nylon mesh, the resulting suspension was centrifuged for 7 min at 200×*g* and then resuspended in DMEM supplemented with 12.5% (v/v) heat-inactivated fetal calf serum (FCS). Cells were plated on poly-L-ornithine-precoated (p-L-Orn) flasks and incubated at 37 °C, in a humid atmosphere containing 5% (v/v) CO_2. Culture medium was changed after 3 days and every 2 days thereafter. The initial mixed glial cultures, grown for 9 to 11 days, were placed on a rotary shaker at 37 °C for 3 h to remove loosely attached macrophages. Oligodendrocyte progenitors and microglia were detached from the astrocyte-like matrix following shaking for 18 h at 260 rpm. After filtration, cells were plated on a plastic surface for 3 h. In these conditions, microglia attached and oligodendrocyte progenitors remaining in suspension were separated and plated on multi-well dishes precoated with poly-D-lysine at an approximate density of $1.5 \times 10^3/cm^2$. Cultures were maintained in serum-free medium (SFM) containing 2.5 ng/ml human recombinant platelet derived growth factor-AA (PDGF-AA) and 2.5 ng/ml basic fibroblast growth factor (b-FGF; PeproTech Inc.) to stimulate proliferation, and medium was changed every 2 days. Ninety-five percent of the cells reacted positively with monoclonal antibody A2B5 (ATCC), a marker for oligodendrocyte progenitors. Progenitor cultures were differentiated to oligodendrocytes in SFM without PDGF-AA and b-FGF, which was supplemented with 3% (v/v) calf serum after day 3. Mature oligodendrocyte cultures were more than 90% myelin basic protein (MBP)-positive cells. Microglial cells, identified by expression of complement type-3 (Monoclonal anti-complement receptor C3b (OX-42); Serotec Inc.), were subplated on p-L-Orn-coated dishes at $1.5 \times 10^3/cm^2$ and were maintained in DMEM with 10% (v/v) FCS. Secondary cultures of astrocytes were placed on p-L-Orn-coated dishes and DMEM with 10% (v/v) FCS after trypsinization of the cells remaining on the flasks.

Cortical and hippocampal cell cultures

Embryos at 16 to 18 days of gestation were removed from pregnant anesthetized Sprague–Dawley rats or BALB/c mice. Cortical or hippocampal cell cultures were obtained following the modified methods of Brewer et al. (1993). Cells were dissected in HBSS without Ca^{2+} and Mg^{2+}, supplemented with 1.0 mM sodium pyruvate and 10 mM HEPES. Individual cells were isolated by trituration in the same medium then diluted with 2 vol of HBSS with Ca^{2+} and Mg^{2+}. Supernatants were then transferred to a 15-ml tube and centrifuged for 1 min at 1000 × *g*. The pellets were resuspended in 1 ml HBSS per brain. Cells were grown on glass coverslips, pretreated with poly-D-lysine and plated at approximately $5 \times 10^5/cm^2$. To obtain enriched neuronal cell cultures, cells were plated in neurobasal medium (Invitrogen) supplemented with 0.5 mM L-glutamine, 25 μM glutamate and B27 supplement (Invitrogen). After 4 days, medium was replaced with Neurobasal/B27 without glutamate. To obtain mixed glial cell cultures, cells were plated in DMEM medium supplemented with 10% (v/v) FCS, neurons could not survive in these conditions.

Infection of cells cultures and infectious virus assays

Almost pure (more than 90%) rat glial cultures were infected with HCoV-OC43 ATCC at a MOI of approximately 50, and DRG-N or DRG-N/SC at a MOI of approximately 10, then incubated for 2 h at 37 °C, washed in warm PBS, and incubated at 37 °C. Supernatants were collected in the first 8 days post-infection and also at 2 or 3 weeks post-infection for glial cell cultures. Since hippocampal or cortical cultures were highly susceptible to HCoV-OC43 infection, the MOI used were reduced, and cell cultures were rather infected at an MOI of 1, with HCoV-OC43 ATCC, HCoV-OC43 Paris, or MHV-A59, incubated at 37 °C for 2 h, then washed in warm PBS and incubated at 37 °C. Supernatants were collected at 1, 2, 3, 4, and 5 days post-infection. Collected supernatants were centrifuged for 5 min at 1000 × *g* and then immediately frozen at −80 °C and stored until assayed. The extracts were processed for the presence and quantification of infectious virus by an indirect immunoperoxidase assay, as previously described (Jacomy and Talbot, 2003).

TNF-α detection

The quantitative determination of mouse tumor necrosis factor alpha (TNF-α) concentrations in cell cultures supernatants was determined using the mouse TNF-α Detection Kit Quantine (R&D Systems, Inc.). Supernatants from infected and noninfected cell cultures were collected at 18 and 24 h post-infection, centrifuged to remove cell debris, and store at −80 °C until used. The extracts were processed for the presence and quantification of TNF-α. Each value was determined using at least 3 samples collected from triplicate wells and assayed in duplicate as recommended by the manufacturer.

Immunofluorescence staining

For detection of surface antigens, unfixed cells were incubated with monoclonal antibodies A2B5 or OX-42 in culture medium. After rinsing with culture medium, the cells were incubated for 20 min with fluorescent secondary antibodies (Alexa Fluor 488 F(ab′)2 fragments of goat anti-mouse IgG (H+L); Molecular Probes) at a 1/1500 dilution.

To visualize viral antigens and cell markers, cultures were washed with warm sterile PBS, then fixed with 4% (v/v) paraformaldehyde at 4 °C, for 30 min. After washing, cells were permeabilized with 100% methanol at −20 °C for 5 min, washed again in PBS, then incubated 2 h with primary antibodies, as previously described (Robertson et al., 2001). For viral antigens, we used 1/1000 dilutions of ascites fluid of the 4-E11.3 hybridoma that secretes monoclonal antibodies specific for the nucleocapsid protein of the serologically related hemagglutinating encephalomyelitis virus of pigs (Bonavia et al., 1997) or a rabbit-anti-BCoV antiserum specific for the nucleocapsid protein of the serologically related bovine coronavirus at 1/500 dilution (Michaud and Dea, 1993). Astrocytes were identified with a rabbit-anti-glial-fibrillary acidic protein antibody (GFAP) obtained from DAKO and diluted 1/500 and neurons by MAP1b antibodies (MAP5, clone AA6, mouse ascites fluid; Sigma) or monoclonal NFH antibody N52 (Sigma), all at a dilution of 1/1000. Microglial cells and oligodendrocytes were identified by OX-42 antibody at 1/1000 or rabbit anti-MBP at 1/500, respectively, and activated microglia by an ascites fluid of the rat Mac-2 antibody (ATCC). Apoptotic cells were revealed by antibodies to active caspase-3 at a dilution of 1/50 (rabbit anti-human/mouse active caspase-3 antibodies; R&D Systems, Inc.). After several washes in PBS, cell coverslips were incubated for 1 h at 37 °C in the dark with one or a combination of immunofluorescent secondary antibodies; Alexa Fluor 488 (Molecular Probes) at a dilution of 1/1500; TRITC anti-rabbit IgG at 1/500; TRITC anti-mouse IgG, IgA, IgM at 1/1000 or FITC $(Fab')_2$ anti-IgG rabbit at 1/1000 (all from Cappel Organon Technika Corp.). Then after 3 washes in water, cells were incubated in 4,6-diamidino-2-phenylindole dihydrochloride (DAPI; Polysciences Inc.) at a 1/100 dilution for 5 min. After final washes in water, coverslips from each well were removed and mounted on microscope slides in Immuno-mount and observed under a fluorescence microscope.

Animal model

Forty BALB/c mice (MHV-seronegative female; Jackson Laboratories), aged 21 days post-natal (DPN) were inoculated by intracerebral (IC) route, using 10 μl containing $10^{4.5}$ $TCID_{50}$ of HCoV-OC43 as previously described (Jacomy and Talbot, 2003). Twelve control mice received an intracerebral inoculation of 10 μl of HRT-18 cell culture medium. Five infected and two control mice were sacrificed for TUNEL staining at 11 days post-infection. Twenty-nine of the remaining 35 mice survived to acute encephalitis and were processed for viral RNA detection and histological examination. Eight mice were sacrificed at 6 months post-infection and the remaining 21 animals at the end of behavioral observations. Control mice were processed in parallel.

Preparation of RNA and nested-RT-PCR assay

Total brain RNA was extracted by homogenization in Trizol (GibcoBRL, Burlington, CA). For RT-PCR, one pair of HCoV-OC43 primers was designed to amplify a region of 305 nucleotides (primers O1 and O3) of the gene coding for the N protein (Arbour et al., 1999). Approximately 5 μg of RNA was reversed transcribed with Expand Moloney murine leukemia virus reverse transcriptase (GibcoBRL), and the cDNA products were amplified by 30 PCR amplification cycles as previously described (Jacomy and Talbot, 2003). A nested PCR was performed on these RT-PCR amplicons using primers O1.1–O3.1 (Arbour et al., 2000): 40 amplification cycles were performed. Ten microliters of RT-PCR and nested RT-PCR products was loaded onto a 1.2% (w/v) agarose gel containing 5 μl ethidium bromide.

TUNEL assays in brain slices

The In Situ Cell Death Detection FITC Kit (Roche Molecular Diagnostics) was used for TUNEL (transferase dUTP nick end labeling) assays. Fluorescent double labeling of brain slices with antibody to infected cells was performed in conjunction with the TUNEL assay to enable correlation of TUNEL-positive cells with the presence of a viral infection. Briefly, mice were intracardially perfused with 4% (v/v) paraformaldehyde, as previously described (Jacomy and Talbot, 2003). Brains were paraffin embedded and sectioned longitudinally. Sections were collected on slides, deparaffined, and were incubated with primary antibodies for viral antigens and for TUNEL staining, as recommended by the manufacturer.

Immunohistochemistry

At 6 months or 1 year post-infection, mice were perfused, and coronal or sagittal brain sections were prepared at a thickness of 40 μm with a Lancer Vibratome. Serial sections were collected and were then incubated overnight with primary antibodies, as previously described (Jacomy and Talbot, 2003). For viral antigens, we used 1/1000 dilutions of ascites fluids of the 4-E11.3 hybridoma (Bonavia et al., 1997). Astrocytes were

identified with a rabbit–anti-glial-fibrillary acidic protein antibody (GFAP, DAKO) diluted 1/500, and microglia/macrophages by an ascites fluid of the rat Mac-2 antibody (ATCC) diluted 1/1000. Two sets of sections were stained with the classical Cresyl violet stain and hematoxylin–eosin, respectively.

Behavioral observation profile

Mice were picked-up by the tail and held suspended for a maximum of 1 min. Clasping of the four limbs was scored as either present or absent (Ordway et al., 1997). Mice presenting limb clasping were called symptomatic mice. Locomotor activity was quantitatively observed in an open field testing. A Plexiglass plate measuring 45 × 45 cm was divided with 3 lines each separated by 15 cm. The animals were left in the center of the Plexiglass plate for 5 min to explore the novel environment. Activity was recorded by measuring the number of crossing of lines, when a mouse removed all four paws from one square and entered another. Mice were assigned to three experimental groups: control (10 mice), asymptomatic (14 mice), and symptomatic (7 mice). A decrease in number of counts was considered as a decrease in locomotor activity. The Plexiglass was carefully cleaned between tests. Sniffing and sifting were also observed (Clifford et al., 2002).

Acknowledgments

We thank Marc Desforges, INRS-Institut Armand-Frappier, for the critical review of the manuscript and Francine Lambert for the excellent technical assistance. We also thank Marie Désy, INRS-Institut Armand-Frappier, for the statistical analysis. This work was supported by Grant No. MT-9203 from the Canadian Institutes of Health Research (Institute of Infection and Immunity) to Pierre J. Talbot, who is the holder of a Tier-I Canada Research Chair in Neuroimmunovirology.

References

Almazan, G., Afar, D.E., Bell, J.C., 1993. Phosphorylation and disruption of intermediate filament proteins in oligodendrocyte precursor cultures treated with calyculin A. J. Neurosci. Res. 36, 163–172.

Arbour, N., Côté, G., Lachance, C., Tardieu, M., Cashman, N.R., Talbot, P.J., 1999. Acute and persistent infection of human neural cell lines by human coronavirus OC43. J. Virol. 73, 3338–3350.

Arbour, N., Day, R., Newcombe, J., Talbot, P.J., 2000. Neuroinvasion by human respiratory coronaviruses and association with multiple sclerosis. J. Virol. 74, 8913–8921.

Bonavia, A., Arbour, N., Wee Yong, V., Talbot, P.J., 1997. Infection of primary cultures of human neural cells by human coronavirus 229E and OC43. J. Virol. 71, 800–806.

Brewer, G.J., Torricelli, J.R., Evege, E.K., Price, P.J., 1993. Optimized survival of hippocampal neurons in B27-supplemented neurobasal, a new serum-free medium combination. J. Neurosci. Res. 35, 567–576.

Burks, J.S., DeVald, B.L., Jankovsky, L.D., Gerdes, J.C., 1980. Two coronaviruses isolated from central nervous system tissue of multiple sclerosis patients. Science 209, 933–934.

Chen, B.P., Lane, T.E., 2002. Lack of nitric oxide synthase type 2 (NOS2) results in reduced neuronal apoptosis and mortality following mouse hepatitis virus infection of the central nervous system. J. NeuroVirol. 8, 58–63.

Clifford, J.J., Drago, J., Natoli, A.L., Wong, J.Y., Kinsella, A., Waddington, J.L., Vaddadi, K.S., 2002. Essential fatty acids given from conception prevent topographies of motor deficit in a transgenic model of Huntington's disease. Neuroscience 109, 81–88.

Collins, A.R., 1995. Interferon gamma potentiates human coronavirus OC43 infection of neuronal cells by modulation of HLA class I expression. Immunol. Invest. 24, 977–986.

Connor, T.J., Leonard, B.E., 1998. Depression, stress and immunological activation: the role of cytokines in depressive disorders. Life Sci. 7, 583–606.

Côté, F., Collard, J.-F., Julien, J.-P., 1993. Progressive neuropathy in transgenic mice expressing the human neurofilament heavy gene: a mouse model for amyotrophic lateral sclerosis. Cell 73, 35–46.

Daniel, C., Talbot, P.J., 1987. Physico-chemical properties of murine hepatitis virus, strain A59. Arch. Virol. 96, 241–248.

DeBiasi, R.L., Kleinschmidt-DeMasters, B.K., Richardson-Burns, S., Tyler, K.L., 2002. Central nervous system apoptosis in human herpes simplex virus and cytomegalovirus encephalitis. J. Infect. Dis. 186, 1547–1557.

Ding, Y., He, L., Zhang, Q., Huang, Z., Che, X., Hou, J., Wang, H., Shen, H., Qiu, L., Li, Z., Geng, J., Cai, J., Han, H., Li, X., Kang, W., Weng, D., Liang, P., Jiang, S., 2004. Organ distribution of severe acute respiratory syndrome (SARS) associated coronavirus (SARS-CoV) in SARS patients: implications for pathogenesis and virus transmission pathways. J. Pathol. 203, 622–630.

Garden, G.A., 2002. Microglia in human immunodeficiency virus-associated neurodegeneration. Glia 40, 240–251.

Giasson, B.I., Mushynski, W.E., 1996. Aberrant stress-induced phosphorylation of perikaryal neurofilaments. J. Biol. Chem. 271, 30404–30409.

Gimsa, U., Peter, S.V., Lehmann, K., Bechmann, I., Nitsch, R., 2000. Axonal damage induced by invading T cells in organotypic central nervous system tissue in vitro: involvement of microglial cells. Brain Pathol. 10, 365–377.

Glass, W.G., Subbarao, K., Murphy, B., Murphy, P.M., 2004. Mechanisms of host defense following severe acute respiratory syndrome-coronavirus (SARS-CoV) pulmonary infection of mice. J. Immunol. 173, 4030–4039.

Guidotti, L.G., Chisari, F.V., 2001. Noncytolytic control of viral infections by the innate and adaptive immune response. Annu. Rev. Immunol. 19, 65–91.

Guy, J., Hendrich, B., Holmes, M., Martin, J.E., Bird, A., 2001. A mouse Mecp2-null mutation causes neurological symptoms that mimic Rett syndrome. Nat. Genet. 27, 322–326.

Herbein, G., O'Brien, W.A., 2000. Tumor necrosis factor (TNF)-alpha and TNF receptors in viral pathogenesis. Proc. Soc. Exp. Biol. Med. 223, 241–257.

Hung, E.C., Chim, S.S., Chan, P.K., Tong, Y.K, Ng, E.K., Chiu, R.W., Leung, C.B., Sung, J.J., Tam, J.S., Lo, Y.M., 2003. Detection of SARS coronavirus RNA in the cerebrospinal fluid of a patient with severe acute respiratory syndrome. Clin. Chem. 49, 2108–2109.

Jacomy, H., Talbot, P.J., 2003. Vacuolating encephalitis in mice infected by human coronavirus OC43. Virology 315, 20–33.

Kimura, T., Griffin, D.E., 2003. Extensive immune-mediated hippocampal damage in mice surviving infection with neuroadapted Sindbis virus. Virology 311, 28–39.

Kolson, D.L., 2002. Neuropathogenesis of central nervous system HIV-1 infection. Clin. Lab. Med. 22, 703–717.

Lau, K.K., Yu, W.C., Chu, C.M., Lau, S.T., Sheng, B., Yuen, K.Y., 2004. Possible central nervous system infection by SARS coronavirus. Emerging Infect. Dis. 10, 342–344.

Li, Y., Fu, L., Gonzales, D.M., Lavi, E., 2004. Coronavirus neurovirulence correlates with the ability of the virus to induce proinflammatory cytokine signals from astrocytes and microglia. J. Virol. 78, 3398–3406.

McCarthy, K.D., de Vellis, J., 1980. Preparation of separate astroglial and oligodendroglial cell cultures from rat cerebral tissue. J. Cell Biol. 85, 890–902.

McGeer, P.L., McGeer, E.G., 2002. Local neuroinflammation and the progression of Alzheimer's disease. J. NeuroVirol. 8, 529–538.

McIntosh, K., 1996. In: Fields, B.N., Knipe, D.M., Howley, P.H. (Eds.), Virology, 3rd ed. Raven Press, New York, pp. 1095–1103.

Michaud, L., Dea, S., 1993. Characterization of monoclonal antibodies to bovine enteric coronavirus and antigenic variability among Quebec isolates. Arch. Virol. 131, 455–465.

Mollinedo, F., Gajate, C., 2003. Microtubules, microtubule-interfering agents and apoptosis. Apoptosis 8, 413–450.

Mounir, S., Talbot, P.J., 1992. Sequence analysis of the membrane protein gene of human coronavirus OC43 and evidence for *O*-glycosylation. J. Gen. Virol. 73, 2731–2736.

Murray, R.S., Brown, B., Brian, D., Cabirac, G.F., 1992. Detection of coronavirus RNA and antigen in multiple sclerosis brain. Ann. Neurol. 31, 525–533.

Myint, S.H., 1994. Human coronavirus—A brief review. Rev. Med. Virol. 4, 35–46.

Nakagaki, K., Nakagaki, K., Taguchi, F., 2005. Receptor-independent spread of a highly neurotropic murine coronavirus JHMV strain from initially infected microglial cells in mixed neural cultures. J. Virol. 79, 6102–6110.

Nakai, Y., Itoh, M., Mizuguchi, M., Ozawa, H., Okazaki, E., Kobayashi, Y., Takahashi, M., Ohtani, K., Ogawa, A., Narita, M., Togashi, T., Takashima, S., 2003. Apoptosis and microglial activation in influenza encephalopathy. Acta Neuropathol. 105, 233–239.

Nicholson, D.W., Ali, A., Thornberry, N.A., Vaillancourt, J.P., Ding, C.K., Gallant, M., Gareau, Y., Griffin, P.R., Labelle, M., Lazebnik, Y.A., Munday, N.A., Raju, S.M., Smulson, M.E., Yamin, T.-T., Yu, V.L., Miller, D.K., 1995. Identification and inhibition of the ICE/CED-3 protease necessary for mammalian apoptosis. Nature 376, 37–43.

Nie, Q.H., Luo, X.D., Zhang, J.Z., Su, Q., 2003. Current status of severe acute respiratory syndrome in China. World J. Gastroenterol. 9, 1635–1645.

Ochs, S., Pourmand, R., Jersild Jr., R.A., 1996. Origin of beading constrictions at the axolemma: presence in unmyelinated axons and after beta,beta'-iminodipropionitrile degradation of the cytoskeleton. Neuroscience 70, 1081–1096.

Ordway, J.M., Tallaksen-Greene, S., Gutekunst, C.A., Bernstein, E.M., Cearley, J.A., Wiener, H.W., Dure IV, L.S., Lindsey, R., Hersch, S.M., Jope, R.S., Albin, R.L., Detloff, P.J., 1997. Ectopically expressed CAG repeats cause intranuclear inclusions and a progressive late onset neurological phenotype in the mouse. Cell 91, 753–763.

Padgett, D.A., Glaser, R., 2003. How stress influences the immune response. Trends Immunol. 24, 444–448.

Pearson, J., Mims, C.A., 1985. Differential susceptibility of cultured neural cells to the human coronavirus OC43. J. Virol. 53, 1016–1019.

Peiris, J.S.M., Laib, S.T., Poona, L.L.M., Guana, Y., Yamd, L.Y.C., Limc, W., Nichollsa, J., Yeee, W.K.S., Yanb, W.W., Cheungd, M.T., Chenga, C.C., Chana, K.H., Tsangf, D.N.C., Yungd, R.W.H., Ngb, T.K., Yuen, K.Y., SARS study group, 2003. Coronavirus as a possible cause of severe acute respiratory syndrome. Lancet 19, 1319–1325.

Reddy, P.H., Williams, M., Charles, V., Garrett, L., Pike-Buchanan, L., Whetsell Jr., W.O., Miller, G., Tagle, D.A., 1998. Behavioural abnormalities and selective neuronal loss in HD transgenic mice expressing mutated full-length HD cDNA. Nat. Genet. 20, 198–202.

Rempel, J.D., Quina, L.A., Blakely-Gonzales, P.K., Buchmeier, M.J., Gruol, D.L., 2005. Viral induction of central nervous system innate immune responses. J. Virol. 79, 4369–4381.

Rest, J.S., Mindell, D.P., 2003. SARS associated coronavirus has a recombinant polymerase and coronaviruses have a history of host-shifting. Infect. Genet. Evol. 3, 219–225.

Resta, S., Luby, J.P., Rosenfeld, C.R., Siegel, J.D., 1985. Isolation and propagation of a human enteric coronavirus. Science 229, 978–981.

Riski, N., Hovi, T., 1980. Coronavirus infections of man associated with diseases other than the common cold. J. Med. Virol. 6, 259–265.

Robertson, J., Beaulieu, J.M., Doroudchi, M.M., Durham, H.D., Julien, J.-P., Mushynski, W.E., 2001. Apoptotic death of neurons exhibiting peripherin aggregates is mediated by the proinflammatory cytokine tumor necrosis factor-alpha. J. Cell Biol. 155, 217–226.

Roediger, B., Armati, P.J., 2003. Oxidative stress induces axonal beading in cultured human brain tissue. Neurobiol. Dis. 13, 222–229.

Rozmyslowicz, T., Majka, M., Kijowski, J., Murphy, S.L., Conover, D.O., Poncz, M., Ratajczak, J., Gaulton, G.N., Ratajczak, M.Z., 2003. Platelet- and megakaryocyte-derived microparticles transfer CXCR4 receptor to CXCR4-null cells and make them susceptible to infection by X4-HIV. AIDS 17, 33–42.

Rubio, N., Martin-Clemente, B., Lipton, H.L., 2003. High-neurovirulence GDVII virus induces apoptosis in murine astrocytes through tumor necrosis factor (TNF)-receptor and TNF-related apoptosis-inducing ligand. Virology 311, 366–375.

Schwartz, T., Fu, L., Lavi, E., 2002. Differential induction of apoptosis in demyelinating and nondemyelinating infection by mouse hepatitis virus. J. NeuroVirol. 8, 392–399.

Shi, B., Raina, J., Lorenzo, A., Busciglio, J., Gabuzda, D., 1998. Neuronal apoptosis induced by HIV-1 Tat protein and TNF-alpha: potentiation of neurotoxicity mediated by oxidative stress and implications for HIV-1 dementia. J. NeuroVirol. 4, 281–290.

Sizun, J., Yu, M.W., Talbot, P.J., 2000. Survival of human coronaviruses 229E and OC43 in suspension and after drying on surfaces: a possible source of hospital-acquired infections. J. Hosp. Infect. 46, 55–60.

Snijder, E.J., Bredenbeek, P.J., Dobbe, J.C., Thiel, V., Ziebuhr, J., Poon, L.L., Guan, Y., Rozanov, M., Spaan, W.J., Gorbalenya, A.E., 2003. Unique and conserved features of genome and proteome of SARS-coronavirus, an early split-off from the coronavirus group 2 lineage. J. Mol. Biol. 331, 991–1004.

Stewart, J.N., Mounir, S., Talbot, P.J., 1992. Human coronavirus gene expression in the brains of multiple sclerosis patients. Virology 191, 502–505.

St-Jean, J.R., Jacomy, H., Desforges, M., Vabret, A., Freymuth, F., Talbot, P.J., 2004. Human respiratory coronavirus OC43: genetic stability and neuroinvasion. J. Virol. 78, 8824–8834.

Sun, N., Perlman, S., 1995. Spread of a neurotropic coronavirus to spinal cord white matter via neurons and astrocytes. J. Virol. 69, 633–641.

Talley, A.K., Dewhurst, S., Perry, S.W., Dollard, S.C., Gummuluru, S., Fine, S.M., New, D., Epstein, L.G., Gendelman, H.E., Gelbard, H.A., 1995. Tumor necrosis factor alpha-induced apoptosis in human neuronal cells: protection by the antioxidant *N*-acetylcysteine and the genes bcl-2 and crmA. Mol. Cell. Biol. 15, 2359–2366.

Wu, G.F., Perlman, S., 1999. Macrophage infiltration, but not apoptosis, is correlated with immune-mediated demyelination following murine infection with a neurotropic coronavirus. J. Virol. 73, 8771–8780.

Xu, J., Zhong, S., Liu, J., Li, L., Li, Y., Wu, X., Li, Z., Deng, P., Zhang, J., Zhong, N., Ding, Y., Jiang, Y., 2005. Detection of severe acute respiratory syndrome coronavirus in the brain: potential role of the chemokine mig in pathogenesis. Clin. Infect. Dis. 41, 1089–1096.

Yamamoto, A., Lucas, J.J., Hen, R., 2000. Reversal of neuropathology and motor dysfunction in a conditional model of Huntington's disease. Cell 101, 57–66.

Yeh, E.A., Collins, A., Cohen, M.E., Duffner, P.K., Faden, H., 2004. Detection of coronavirus in the central nervous system of a child with acute disseminated encephalomyelitis. Pediatrics 113, 73–76.

Yokomori, K., Lai, M.M., 1992. The receptor for mouse hepatitis virus in the resistant mouse strain SJL is functional: implications for the requirement of a second factor for viral infection. J. Virol. 66, 6194–6199.